

Search for anomalous four-jet events in e^+e^- annihilation at $\sqrt{s} = 130-172$ GeV

M. Acciarri, O. Adriani, M. Aguilar-Benitez, S. Ahlen, J. Alcaraz, G. Alemanni, J. Allaby, A. Aloisio, G. Alverson, M G. Alviggi, et al.

► **To cite this version:**

M. Acciarri, O. Adriani, M. Aguilar-Benitez, S. Ahlen, J. Alcaraz, et al.. Search for anomalous four-jet events in e^+e^- annihilation at $\sqrt{s} = 130-172$ GeV. Physics Letters B, Elsevier, 1997, 411, pp.330-338. in2p3-00023162

HAL Id: in2p3-00023162

<http://hal.in2p3.fr/in2p3-00023162>

Submitted on 16 Nov 1998

HAL is a multi-disciplinary open access archive for the deposit and dissemination of scientific research documents, whether they are published or not. The documents may come from teaching and research institutions in France or abroad, or from public or private research centers.

L'archive ouverte pluridisciplinaire **HAL**, est destinée au dépôt et à la diffusion de documents scientifiques de niveau recherche, publiés ou non, émanant des établissements d'enseignement et de recherche français ou étrangers, des laboratoires publics ou privés.

**Search for anomalous four-jet events in e^+e^-
annihilation at $\sqrt{s} = 130 - 172$ GeV**

L3 Collaboration

Abstract

A study of hadronic events with high jet-multiplicity is performed using the data sample collected by the L3 experiment at LEP at $\sqrt{s} = 130 - 172$ GeV. The observed event rates agree with the Standard Model predictions and upper limits are set on the production cross section of pairs of heavy particles that decay hadronically.

Submitted to *Phys. Lett. B*

1 Introduction

The increase in energy of the LEP accelerator opens new possibilities to investigate physics beyond the Standard Model. Several of these possibilities, like supersymmetric Higgs production and R-parity violation processes in Supersymmetry [1], are characterized by topologies with a high number of jets and no missing energy. The report from the ALEPH collaboration [2] of anomalous four-jet production has given additional motivation for the search in these channels.

In this paper we report on a search for anomalous four-jet events at $\sqrt{s} = 130 - 172$ GeV. The associated production of hadronically decaying particles (that is the process $e^+e^- \rightarrow XY \rightarrow q\bar{q} q\bar{q}$) would show up as a resonance in the distribution of the invariant mass of the two pairs of jets. The choice among the three possible pairings of the jets depends on the signal searched for. In the hypothesis $M_X = M_Y$ the combination where the difference between the two reconstructed masses is the smallest is considered, while in case the two masses are allowed to be different the other combinations are also used.

2 Data Reconstruction and Monte Carlo samples

The data collected by the L3 experiment during the three runs of LEP at $\sqrt{s} = 130 - 140$ GeV (herein referred to as 133 GeV run) in 1995, 161 GeV and 170 - 172 GeV (herein referred to as 172 GeV run) in 1996 corresponding to an integrated luminosity of $L=5.0 \text{ pb}^{-1}$, 10.9 pb^{-1} and 10.3 pb^{-1} respectively are analysed.

A detailed description of the L3 detector and its performance is given in Reference [3]. Hadronic events are reconstructed using information from all subdetectors. In particular the energy of the event is obtained taking into account the energy deposition in the electromagnetic and hadronic calorimeters and the charged particles momenta measured by the central tracking chamber and the muon chambers.

In order to evaluate the expectations from Standard Model processes, Monte Carlo (MC) event samples of $q\bar{q}(\gamma)$, $e^+e^-q\bar{q}$, $Z/\gamma^*Z/\gamma^*$ were produced using PYTHIA [4] and W^+W^- using KORALW [5]. As a reference reaction to evaluate the efficiency on a possible signal, a sample of MC events $e^+e^- \rightarrow hA \rightarrow \bar{b}b\bar{b}b$ was generated with PYTHIA for several Higgs bosons h and A masses in the range from 30 to 130 GeV. All events were then fully simulated in the L3 detector using the GEANT library [6].

3 Analysis

3.1 Selection of four-jet events

The main sources of production of four-jet events in the Standard Model are hard gluon emission or jet misreconstruction in hadronic events and, at $\sqrt{s} \geq 161$ GeV, W and Z pair production. The separate contributions at the different energies are shown in table 1. The selection of four-jet events is divided in the following steps:

- High Multiplicity Requirement:
Events are required to have at least 10 tracks and 30 calorimetric clusters. In addition the visible energy is required to be greater than 70% of the center-of-mass energy.
- Four-Jet Criteria:
Events consistent with radiative return to the Z ($e^+e^- \rightarrow Z\gamma \rightarrow q\bar{q} \gamma$) are rejected by

process	$\sqrt{s} = 130$ GeV	$\sqrt{s} = 136$ GeV	$\sqrt{s} = 161$ GeV	$\sqrt{s} = 172$ GeV
$e^+e^- \rightarrow q\bar{q}$	336	280	149	124
$e^+e^- \rightarrow WW$	0.07	0.11	3.24	12.2
$e^+e^- \rightarrow Z/\gamma^*Z/\gamma^*$	0.50	0.47	0.46	0.43

Table 1: Cross sections (pb) of processes contributing to four-jet events production.

requiring the effective center-of-mass energy ($\sqrt{s'}$) to be greater than $0.87\sqrt{s}$. If the radiative photon is not detected in the calorimeters $\sqrt{s'}$ is computed from the jet angles with the assumption that one photon has escaped in the beam pipe.

Jets are then reconstructed using the Durham [7] algorithm and events are rejected if they have less than four jets for the jet resolution parameter $y_{cut} = 0.008$. In addition none of the jets must contain electromagnetic energy in excess of 85% of the jet energy. Events satisfying these requirements are reconstructed again but with a variable y_{cut} chosen in order to have exactly four jets.

A kinematic fit that requires four momentum conservation is applied to improve the energy and angular resolution. This constraint induces a negative correlation between the two jet pair masses such that the sum of the masses has a better resolution than the difference. Thus in the following the sum of the reconstructed masses of the two combinations with the smallest difference of masses (called respectively ΣM_1 and ΣM_2) are shown.

- Jet Quality Requirements:

Events are rejected if any of the four jets has an energy smaller than $5\%\sqrt{s}$, has no tracks or is within an 8° cone around the beam pipe. After applying these criteria mainly QCD four-jet events and hadronic W decays are expected from Standard Model processes.

- Kinematic Requirements:

QCD four-jet events predominantly consist of two nearly back to back energetic jets and two low energy jets. These events are therefore characterized by a high difference between the most and the least energetic jet ($\Delta_E = E_{max} - E_{min}$) and a maximum angle between jets (θ_{max}) close to 180° . The minimum invariant mass of jet pairs (M_{min}) is small.

Events are therefore required to have $\Delta_E < 0.3\sqrt{s}$, $M_{min} > 0.18\sqrt{s}$ and, for the 161 GeV data, $\cos(\theta_{max}) > -0.95$.

- W Pair Rejection:

W pair events are identified using a kinematic fit with the assumption that for one possible pairing of the four jets both di-jet invariant masses are equal to the W mass. Events are rejected if the χ^2 of this fit is small.

The number of events expected from Standard Model processes, the efficiency on the signal, for the mass points $M_h = M_A = 55$ or 60 GeV at 133 and $161 - 172$ GeV respectively, and the number of data events observed are shown in table 2. Agreement between data and MC is found at all the stages of the analysis as shown in figure 1. In order to search for signals where the two particles produced do not have the same masses both ΣM_1 and ΣM_2 are plotted in figure 2. No significant deviation from the Standard Model expectations is found in these distributions.

Set of cuts	N_{data}	N_{ex}	$\epsilon_s(\%)$
$\sqrt{s} = 130 - 140$ GeV			
High Multiplicity	1032	934±4	96.7±0.6
Four Jets	24	23.4±1.0	58.6±1.6
Jet Quality	19	19.3±0.9	57.6±1.6
Kinematics	14	9.6±0.6	48.6±1.7
$\sqrt{s} = 161$ GeV			
High Multiplicity	827	790±2	93.6±0.5
Four Jets	28	32.9±0.5	56.5±1.6
Jet Quality	24	29.2±0.4	55.1±1.5
Kinematics	7	10.0±0.3	35.5±1.5
WW rejection	6	7.9±0.2	33.8±1.5
$\sqrt{s} = 170 - 172$ GeV			
High Multiplicity	623	610 ±3	92.1 ±0.9
Four Jets	49	54.8±0.4	52.8 ±1.6
Jet Quality	48	49.8±0.4	50.7 ±1.6
Kinematics	33	36.4±0.2	40.8 ±1.6
WW rejection	14	14.0±0.2	31.1 ±1.4

Table 2: Number of data events observed (N_{data}), number of events expected from Standard Model processes (N_{ex}) and efficiency for an $e^+e^- \rightarrow hA$ signal at different stages of the analysis. The quoted errors are due to MC statistics only.

3.2 Experimental checks

Several studies using control data samples are carried out to verify the detector performance.

- Return to the Z events:

A sample of radiative return to the Z events with an energetic, isolated photon in the electromagnetic calorimeter is selected. The measured photon energy is required to be within ± 5 GeV of the expected one. These events are reconstructed imposing a three body constraint, assuming that the photon direction is known and leaving its energy free. The measured mass of the hadronic system peaks at the mass of the Z (figure 3a) and the width of the distribution in the data is 3.0 ± 0.2 GeV. There is agreement between data and MC and no shift is observed: the difference between the mean values is 0.2 ± 0.2 GeV. The consistency between data and MC confirms that the evaluation of the sensitivity to the signal using MC samples is correct.

- MC simulation of $e^+e^- \rightarrow hA$:

In order to evaluate the mass resolution for a four-jet signal, the MC sample with $M_A = M_h = 55$ GeV at 133 GeV and $M_A = M_h = 60$ GeV at 161 and 172 GeV respectively were considered. The fit to the distribution of the sum of the masses ΣM_1 (figure 3b) gives a resolution of 2.2 ± 0.2 GeV at $\sqrt{s} = 133$ GeV, 2.5 ± 0.2 at $\sqrt{s} = 161$ GeV and 3.2 ± 0.2 GeV at $\sqrt{s} = 172$ GeV. The mean values of the fits are consistent with the generated mass values within 0.5 GeV.

- WW events at $\sqrt{s} = 172$ GeV:

The distribution of the sum of the di-jet invariant masses ΣM_1 and ΣM_2 at $\sqrt{s} = 172$

GeV before the WW rejection (figure 4) shows a peak around 160 GeV due to W pair production. As a check of the analysis we extract the $e^+e^- \rightarrow W^+W^-$ cross section in a log-likelihood fit to this distribution assuming the Standard Model branching ratio of the W into hadrons. The result $\sigma_{WW} = (10.9 \pm 2.4(stat.))\text{pb}$ is in agreement with the Standard Model prediction of 12.2 pb.

- Complementary analyses:

In addition several analyses with different energy flows and kinematic rescalings have been performed yielding results similar to the one described in section 3.1.

In particular an analysis close to the one published by the ALEPH collaboration [2] with similar efficiencies and resolutions was performed. The number of data events selected, the number of events expected from Standard Model processes and the efficiency on a possible signal are reported in table 3. The differences between this analysis and the one described in section 3.1 are in the jet reconstruction, in the di-jet quality requirements and in the WW rejection. For this analysis figure 5 shows the combined plot of ΣM_1 and ΣM_2 for the three running periods after all cuts. Also for this analysis we find good agreement between data and Standard Model expectations.

\sqrt{s} (GeV)	N_{data}	N_{ex}	$\epsilon_s(\%)$
130 – 140	12	8.1 ± 0.6	44.8 ± 1.7
161	7	8.0 ± 0.2	32.2 ± 1.5
170 – 172	14	13.5 ± 0.2	25.7 ± 1.4

Table 3: Number of data events observed (N_{data}), number of events expected from the Standard Model (N_{ex}) and efficiency for the signal $e^+e^- \rightarrow hA$ (ϵ_s) using a selection that follows the one published by ALEPH. Errors are due to MC statistics only.

4 Results

Good agreement is found between our data and the expectations from the Standard Model both in the rate of four-jet events and in their mass spectrum. The DELPHI and OPAL collaborations reported on similar studies on 130 – 140 GeV data [8].

Upper limits on the production cross section of possible new physics in this channel are derived using the events that satisfy the criteria described in section 3.1. The efficiencies calculated from the $e^+e^- \rightarrow hA \rightarrow b\bar{b}b\bar{b}$ MC are assumed. The number of events predicted by the Standard Model is computed in ΣM_1 windows with a half width corresponding to approximately twice the resolution. The central ΣM_1 values of these windows are moved from 90 to 150 GeV in 1 GeV steps. In each window the maximum number of signal events compatible at 95% C.L. with our observation is calculated and converted into a cross section upper limit (σ_{lim}) at each center-of-mass energy (figure 6a-c). The combination of data at different center-of-mass energies is also made, assuming constant signal cross section.

Removing the constraint that the two hadronically decaying particles produced have equal masses, the same procedure is carried out for the sum of the masses selecting jet pairs with mass differences closest to 10 and 20 GeV. As shown in figure 6d the cross section upper limit σ_{lim} ranges between 0.7 and 1.6 pb for $\Sigma M_1 < 140$ GeV.

5 Acknowledgements

We wish to congratulate the CERN accelerator divisions for the successful upgrade of the LEP machine and to express our gratitude for the good performance of the machine. We acknowledge with appreciation the effort of all engineers, technicians and support staff who have participated in the construction and maintenance of this experiment. Those of us who are not from member states thank CERN for its hospitality and help.

References

- [1] M. Carena *et al.* in *Physics at LEP2*, eds. G. Altarelli *et al.*, vol. 1, report CERN 96-01,p.351.;
G.F. Giudice *et al.* in *Physics at LEP2*, eds. G. Altarelli *et al.*, vol. 1, report CERN 96-01,p.465.
- [2] ALEPH Collaboration, D. Buskulic *et al.*, *Zeitschrift für Physik C* **71** (1996) 179.
- [3] L3 Collaboration, B. Adeva *et al.*, *Nucl. Inst. and Meth. A* **289** (1990) 35-102.;
M. Chemarin *et al.*, *Nucl. Instr. and Meth. A* **349** (1994) 345;
M. Acciarri *et al.*, *Nucl. Instr. and Meth. A* **351** (1994) 300;
A. Adam *et al.*, *Nucl. Instr. and Meth. A* **383** (1996) 342;;
G. Basti *et al.*, *Nucl. Instr. and Meth. A* **374** (1996) 293.
- [4] T. Sjöstrand, CERN-TH/7112/93 (1993), revised August 1995;
T. Sjöstrand, *Comp. Phys. Comm.* 82 (1994) 74.
- [5] M. Skrzypek *et al.*, *Comp.Phys.Comm.* **94** (1996) 216;
M. Skrzypek *et al.*, *Phys.Lett.* **B372** (1996) 289.
- [6] The L3 detector simulation is based on GEANT Version 3.15.
See R. Brun *et al.*, “GEANT 3”, CERN DD/EE/84-1 (Revised), September 1987.
- [7] S. Catani *et al.*, *Phys. Lett.* **B 263** (1991) 491;
S. Bethke *et al.*, *Nucl. Phys.* **B 370** (1992) 310.
- [8] DELPHI Collaboration, P. Abreu *et al.*, *Zeitschrift für Physik C* **73** (1996) 1;
OPAL Collaboration, G. Alexander *et al.*, *Zeitschrift für Physik C* **73** (1997) 201.

The L3 Collaboration:

M. Acciarri,²⁹ O. Adriani,¹⁸ M. Aguilar-Benitez,²⁸ S. Ahlen,¹² J. Alcaraz,²⁸ G. Alemani,²⁴ J. Allaby,¹⁹ A. Aloisio,³¹ G. Alverson,¹³ M.G. Alviggi,³¹ G. Ambrosi,²¹ H. Anderhub,⁵¹ V.P. Andreev,^{7,40} T. Angelescu,¹⁴ F. Anselmo,¹⁰ A. Arefiev,³⁰ T. Azemoon,³ T. Aziz,¹¹ P. Bagnaia,³⁹ L. Baksay,⁴⁶ S. Banerjee,¹¹ Sw. Banerjee,¹¹ K. Banicz,⁴⁸ A. Barczyk,^{51,49} R. Barillère,¹⁹ L. Barone,³⁹ P. Bartalini,³⁶ A. Baschirotto,²⁹ M. Basile,¹⁰ R. Battiston,³⁶ A. Bay,²⁴ F. Becattini,¹⁸ U. Becker,¹⁷ F. Behner,⁵¹ J. Berdugo,²⁸ P. Berges,¹⁷ B. Bertucci,³⁶ B.L. Betev,⁵¹ S. Bhattacharya,¹¹ M. Biasini,¹⁹ A. Biland,⁵¹ G.M. Bilei,³⁶ J.J. Blaising,⁴ S.C. Blyth,³⁷ G.J. Bobbink,² R. Bock,¹ A. Böhm,¹ L. Boldizar,¹⁵ B. Borgia,³⁹ D. Bourilkov,⁵¹ M. Bourquin,²¹ S. Braccini,²¹ J.G. Branson,⁴² V. Brigljevic,⁵¹ I.C. Brock,³⁷ A. Buffini,¹⁸ A. Buijs,⁴⁷ J.D. Burger,¹⁷ W.J. Burger,²¹ J. Busenitz,⁴⁶ A. Button,³ X.D. Cai,¹⁷ M. Campanelli,⁵¹ M. Capell,¹⁷ G. Cara Romeo,¹⁰ G. Carlino,³¹ A.M. Cartacci,¹⁸ J. Casaus,²⁸ G. Castellini,¹⁸ F. Cavallari,³⁹ N. Cavallo,³¹ C. Cecchi,²¹ M. Cerrada,²⁸ F. Cesaroni,²⁵ M. Chamizo,²⁸ Y.H. Chang,⁵³ U.K. Chaturvedi,²⁰ S.V. Chekanov,³³ M. Chemarin,²⁷ A. Chen,⁵³ G. Chen,⁸ G.M. Chen,⁸ H.F. Chen,²² H.S. Chen,⁸ X. Chereau,⁴ G. Chiefari,³¹ C.Y. Chien,⁵ L. Cifarelli,⁴¹ F. Cindolo,¹⁰ C. Cividini,¹⁸ I.M. Clare,¹⁷ R. Clare,¹⁷ H.O. Cohn,³⁴ G. Coignet,⁴ A.P. Colijn,² N. Colino,²⁸ V. Commichau,¹ S. Costantini,⁹ F. Cotorobai,¹⁴ B. de la Cruz,²⁸ A. Csilling,¹⁵ T.S. Dai,¹⁷ R.D. Alessandro,¹⁸ R. de Asmundis,³¹ A. Degré,⁴ K. Deiters,⁴⁹ D. della Volpe,³¹ P. Denes,³⁸ F. DeNotaristefani,³⁹ D. DiBitonto,⁴⁶ M. Diemoz,³⁹ D. van Dierendonck,² F. Di Lodovico,⁵¹ C. Dionisi,³⁹ M. Dittmar,⁵¹ A. Dominguez,⁴² A. Doria,³¹ M.T. Dova,² D. Duchesneau,⁴ P. Duinker,² I. Duran,⁴³ S. Dutta,¹¹ S. Easo,³⁶ Yu. Efremenko,³⁴ H. El Mamouni,²⁷ A. Engler,³⁷ F.J. Eppling,¹⁷ F.C. Erné,² J.P. Ernenwein,²⁷ P. Extermann,²¹ M. Fabre,⁴⁹ R. Faccini,³⁹ S. Falciano,³⁹ A. Favara,¹⁸ J. Fay,²⁷ O. Fedin,⁴⁰ M. Felcini,⁵¹ B. Fenyi,⁴⁶ T. Ferguson,³⁷ F. Ferroni,³⁹ H. Fesefeldt,¹ E. Fiandrini,³⁶ J.H. Field,²¹ F. Filthaut,³⁷ P.H. Fisher,¹⁷ I. Fisk,⁴² G. Forconi,¹⁷ L. Fredj,²¹ K. Freudenreich,⁵¹ C. Furetta,²⁹ Yu. Galaktionov,^{30,17} S.N. Ganguli,¹¹ P. Garcia-Abia,⁵⁰ S.S. Gau,¹³ S. Gentile,³⁹ N. Gheordanescu,¹⁴ S. Giagu,³⁹ S. Goldfarb,²⁴ J. Goldstein,¹² Z.F. Gong,²² A. Gougas,⁵ G. Gratta,³⁵ M.W. Gruenewald,⁹ V.K. Gupta,³⁸ A. Gurtu,¹¹ L.J. Gutay,⁴⁸ B. Hartmann,¹ A. Hasan,³² D. Hatzifotiadou,¹⁰ T. Hebbeker,⁹ A. Hervé,¹⁹ W.C. van Hoek,³³ H. Hofer,⁵¹ S.J. Hong,⁴⁵ H. Hoorani,³⁷ S.R. Hou,⁵³ G. Hu,⁵ V. Innocenti,⁹ K. Jenkes,¹ B.N. Jin,⁸ L.W. Jones,³ P. de Jong,¹⁹ I. Josa-Mutuberria,²⁸ A. Kasser,²⁴ R.A. Khan,²⁰ D. Kamrad,⁵⁰ Yu. Kamyshev,³⁴ J.S. Kapustinsky,²⁶ Y. Karyotakis,⁴ M. Kaur,^{20,◇} M.N. Kienzle-Focacci,²¹ D. Kim,³⁹ D.H. Kim,⁴⁵ J.K. Kim,⁴⁵ S.C. Kim,⁴⁵ Y.G. Kim,⁴⁵ W.W. Kinnison,²⁶ A. Kirkby,³⁵ D. Kirkby,³⁵ J. Kirkby,¹⁹ D. Kiss,¹⁵ W. Kittel,³³ A. Klimentov,^{17,30} A.C. König,³³ A. Kopp,⁵⁰ I. Korolko,³⁰ V. Koutsenko,^{17,30} R.W. Kraemer,³⁷ W. Krenz,¹ A. Kunin,^{17,30} P. Ladron de Guevara,²⁸ I. Laktineh,²⁷ G. Landi,¹⁸ C. Lapointe,¹⁷ K. Lassila-Perini,⁵¹ P. Laurikainen,²³ M. Lebeau,¹⁹ A. Lebedev,¹⁷ P. Lebrun,²⁷ P. Lecomte,⁵¹ P. Lecoq,¹⁹ P. Le Coultre,⁵¹ J.M. Le Goff,¹⁹ R. Leiste,⁵⁰ E. Leonardi,³⁹ P. Levchenko,⁴⁰ C. Li,²² C.H. Lin,⁵³ W.T. Lin,⁵³ F.L. Linde,^{2,19} L. Lista,³¹ Z.A. Liu,⁸ W. Lohmann,⁵⁰ E. Longo,³⁹ W. Lu,³⁵ Y.S. Lu,⁸ K. Lübelmeyer,¹ C. Luci,³⁹ D. Luckey,¹⁷ L. Luminari,³⁹ W. Lustermann,⁴⁹ W.G. Ma,²² M. Maity,¹¹ G. Majumder,¹¹ L. Malgeri,³⁹ A. Malinin,³⁰ C. Mañá,²⁸ D. Mangeol,³³ S. Mangla,¹¹ P. Marchesini,⁵¹ A. Marin,¹² J.P. Martin,²⁷ F. Marzano,³⁹ G.G.G. Massaro,² D. McNally,¹⁹ R.R. McNeil,⁷ S. Mele,³¹ L. Merola,³¹ M. Meschini,¹⁸ W.J. Metzger,³³ M. von der Mey,¹ Y. Mi,²⁴ A. Mihul,¹⁴ A.J.W. van Mil,³³ G. Mirabelli,³⁹ J. Mnich,¹⁹ P. Molnar,⁹ B. Monteleoni,¹⁸ R. Moore,³ S. Morganti,³⁹ T. Moulik,¹¹ R. Mount,³⁵ S. Müller,¹ F. Muheim,²¹ A.J.M. Muijs,² S. Nahn,¹⁷ M. Napolitano,³¹ F. Nessi-Tedaldi,⁵¹ H. Newman,³⁵ T. Niessen,¹ A. Nippe,¹ A. Nisati,³⁹ H. Nowak,⁵⁰ Y.D. Oh,⁴⁵ H. Opitez,¹ G. Organtini,³⁹ R. Ostonen,²³ C. Palomares,²⁸ D. Pandoulas,¹ S. Paoletti,³⁹ P. Paolucci,³¹ H.K. Park,³⁷ I.H. Park,⁴⁵ G. Pascual,³⁹ G. Passaleva,¹⁸ S. Patricelli,³¹ T. Paul,¹³ M. Pauluzzi,³⁶ C. Paus,¹ F. Pauss,⁵¹ D. Peach,¹⁹ Y.J. Pei,¹ S. Pensotti,²⁹ D. Perret-Gallix,⁴ B. Petersen,³³ S. Petrak,⁹ A. Pevsner,⁵ D. Piccolo,³¹ M. Pieri,¹⁸ J.C. Pinto,³⁷ P.A. Piroué,³⁸ E. Pistolesi,²⁹ V. Plyaskin,³⁰ M. Pohl,⁵¹ V. Pojidaev,^{30,18} H. Postema,¹⁷ N. Produit,²¹ D. Prokofiev,⁴⁰ G. Rahal-Callot,⁵¹ N. Raja,¹¹ P.G. Rancoita,²⁹ M. Rattaggi,²⁹ G. Raven,⁴² P. Razis,³² K. Read,³⁴ D. Ren,⁵¹ M. Rescigno,³⁹ S. Reucroft,¹³ T. van Rhee,⁴⁷ S. Riemann,⁵⁰ K. Riles,³ A. Robohm,⁵¹ J. Rodin,¹⁷ B.P. Roe,³ L. Romero,²⁸ S. Rosier-Lees,⁴ Ph. Rossetet,²⁴ W. van Rossum,⁴⁷ S. Roth,¹ J.A. Rubio,¹⁹ D. Ruschmeier,⁹ H. Rykaczewski,⁵¹ J. Salicio,¹⁹ E. Sanchez,²⁸ M.P. Sanders,³³ M.E. Sarakinos,²³ S. Sarkar,¹ M. Sassowsky,¹ C. Schäfer,¹ V. Schegelsky,⁴⁰ S. Schmidt-Kaerst,¹ D. Schmitz,¹ P. Schmitz,¹ N. Scholz,⁵¹ H. Schopper,⁵² D.J. Schotanus,³³ J. Schwenke,¹ G. Schwing,¹ C. Sciacca,³¹ D. Sciarino,²¹ L. Servoli,³⁶ S. Shevchenko,³⁵ N. Shivarov,⁴⁴ V. Shoutko,³⁰ J. Shukla,²⁶ E. Shumilov,³⁰ A. Shvorob,³⁵ T. Siedenbueg,¹ D. Son,⁴⁵ A. Sopczak,⁵⁰ B. Smith,¹⁷ P. Spillantini,¹⁸ M. Steuer,¹⁷ D.P. Stickland,³⁸ A. Stone,⁷ H. Stone,³⁸ B. Stoyanov,⁴⁴ A. Straessner,¹ K. Strauch,¹⁶ K. Sudhakar,¹¹ G. Sultanov,²⁰ L.Z. Sun,²² G.F. Susinno,²¹ H. Suter,⁵¹ J.D. Swain,²⁰ X.W. Tang,⁸ L. Tauscher,⁶ L. Taylor,¹³ Samuel C.C. Ting,¹⁷ S.M. Ting,¹⁷ M. Tonutti,¹ S.C. Tonwar,¹¹ J. Tóth,¹⁵ C. Tully,³⁸ H. Tuchscherer,⁴⁶ K.L. Tung,⁸ Y. Uchida,¹⁷ J. Ulbricht,⁵¹ U. Uwer,¹⁹ E. Valente,³⁹ R.T. Van de Walle,³³ G. Vesztegombi,¹⁵ I. Vetlitsky,³⁰ G. Viertel,⁵¹ M. Vivargent,⁴ R. Völkert,⁵⁰ H. Vogel,³⁷ H. Vogt,⁵⁰ I. Vorobiev,³⁰ A.A. Vorobyov,⁴⁰ A. Vorvolakos,³² M. Wadhwa,⁶ W. Wallraff,¹ J.C. Wang,¹⁷ X.L. Wang,²² Z.M. Wang,²² A. Weber,¹ F. Wittgenstein,¹⁹ S.X. Wu,²⁰ S. Wynnhoff,¹ J.Xu,¹² Z.Z. Xu,²² B.Z. Yang,²² C.G. Yang,⁸ X.Y. Yao,⁸ J.B. Ye,²² S.C. Yeh,⁵³ J.M. You,³⁷ An. Zalite,⁴⁰ Yu. Zalite,⁴⁰ P. Zemp,⁵¹ Y. Zeng,¹ Z. Zhang,⁸ Z.P. Zhang,²² B. Zhou,¹² G.Y. Zhu,⁸ R.Y. Zhu,³⁵ A. Zichichi,^{10,19,20} F. Ziegler,⁵⁰

- 1 I. Physikalisches Institut, RWTH, D-52056 Aachen, FRG[§]
III. Physikalisches Institut, RWTH, D-52056 Aachen, FRG[§]
 - 2 National Institute for High Energy Physics, NIKHEF, and University of Amsterdam, NL-1009 DB Amsterdam, The Netherlands
 - 3 University of Michigan, Ann Arbor, MI 48109, USA
 - 4 Laboratoire d'Annecy-le-Vieux de Physique des Particules, LAPP, IN2P3-CNRS, BP 110, F-74941 Annecy-le-Vieux CEDEX, France
 - 5 Johns Hopkins University, Baltimore, MD 21218, USA
 - 6 Institute of Physics, University of Basel, CH-4056 Basel, Switzerland
 - 7 Louisiana State University, Baton Rouge, LA 70803, USA
 - 8 Institute of High Energy Physics, IHEP, 100039 Beijing, China[△]
 - 9 Humboldt University, D-10099 Berlin, FRG[§]
 - 10 University of Bologna and INFN-Sezione di Bologna, I-40126 Bologna, Italy
 - 11 Tata Institute of Fundamental Research, Bombay 400 005, India
 - 12 Boston University, Boston, MA 02215, USA
 - 13 Northeastern University, Boston, MA 02115, USA
 - 14 Institute of Atomic Physics and University of Bucharest, R-76900 Bucharest, Romania
 - 15 Central Research Institute for Physics of the Hungarian Academy of Sciences, H-1525 Budapest 114, Hungary[‡]
 - 16 Harvard University, Cambridge, MA 02139, USA
 - 17 Massachusetts Institute of Technology, Cambridge, MA 02139, USA
 - 18 INFN Sezione di Firenze and University of Florence, I-50125 Florence, Italy
 - 19 European Laboratory for Particle Physics, CERN, CH-1211 Geneva 23, Switzerland
 - 20 World Laboratory, FBLJA Project, CH-1211 Geneva 23, Switzerland
 - 21 University of Geneva, CH-1211 Geneva 4, Switzerland
 - 22 Chinese University of Science and Technology, USTC, Hefei, Anhui 230 029, China[△]
 - 23 SEFT, Research Institute for High Energy Physics, P.O. Box 9, SF-00014 Helsinki, Finland
 - 24 University of Lausanne, CH-1015 Lausanne, Switzerland
 - 25 INFN-Sezione di Lecce and Università Degli Studi di Lecce, I-73100 Lecce, Italy
 - 26 Los Alamos National Laboratory, Los Alamos, NM 87544, USA
 - 27 Institut de Physique Nucléaire de Lyon, IN2P3-CNRS, Université Claude Bernard, F-69622 Villeurbanne, France
 - 28 Centro de Investigaciones Energeticas, Medioambientales y Tecnológicas, CIEMAT, E-28040 Madrid, Spain^b
 - 29 INFN-Sezione di Milano, I-20133 Milan, Italy
 - 30 Institute of Theoretical and Experimental Physics, ITEP, Moscow, Russia
 - 31 INFN-Sezione di Napoli and University of Naples, I-80125 Naples, Italy
 - 32 Department of Natural Sciences, University of Cyprus, Nicosia, Cyprus
 - 33 University of Nijmegen and NIKHEF, NL-6525 ED Nijmegen, The Netherlands
 - 34 Oak Ridge National Laboratory, Oak Ridge, TN 37831, USA
 - 35 California Institute of Technology, Pasadena, CA 91125, USA
 - 36 INFN-Sezione di Perugia and Università Degli Studi di Perugia, I-06100 Perugia, Italy
 - 37 Carnegie Mellon University, Pittsburgh, PA 15213, USA
 - 38 Princeton University, Princeton, NJ 08544, USA
 - 39 INFN-Sezione di Roma and University of Rome, "La Sapienza", I-00185 Rome, Italy
 - 40 Nuclear Physics Institute, St. Petersburg, Russia
 - 41 University and INFN, Salerno, I-84100 Salerno, Italy
 - 42 University of California, San Diego, CA 92093, USA
 - 43 Dept. de Física de Partículas Elementales, Univ. de Santiago, E-15706 Santiago de Compostela, Spain
 - 44 Bulgarian Academy of Sciences, Central Lab. of Mechatronics and Instrumentation, BU-1113 Sofia, Bulgaria
 - 45 Center for High Energy Physics, Korea Adv. Inst. of Sciences and Technology, 305-701 Taejeon, Republic of Korea
 - 46 University of Alabama, Tuscaloosa, AL 35486, USA
 - 47 Utrecht University and NIKHEF, NL-3584 CB Utrecht, The Netherlands
 - 48 Purdue University, West Lafayette, IN 47907, USA
 - 49 Paul Scherrer Institut, PSI, CH-5232 Villigen, Switzerland
 - 50 DESY-Institut für Hochenergiephysik, D-15738 Zeuthen, FRG
 - 51 Eidgenössische Technische Hochschule, ETH Zürich, CH-8093 Zürich, Switzerland
 - 52 University of Hamburg, D-22761 Hamburg, FRG
 - 53 High Energy Physics Group, Taiwan, China
- [§] Supported by the German Bundesministerium für Bildung, Wissenschaft, Forschung und Technologie
[‡] Supported by the Hungarian OTKA fund under contract numbers T14459 and T24011.
^b Supported also by the Comisión Interministerial de Ciencia y Tecnología
[‡] Also supported by CONICET and Universidad Nacional de La Plata, CC 67, 1900 La Plata, Argentina
[◇] Also supported by Panjab University, Chandigarh-160014, India
[△] Supported by the National Natural Science Foundation of China.

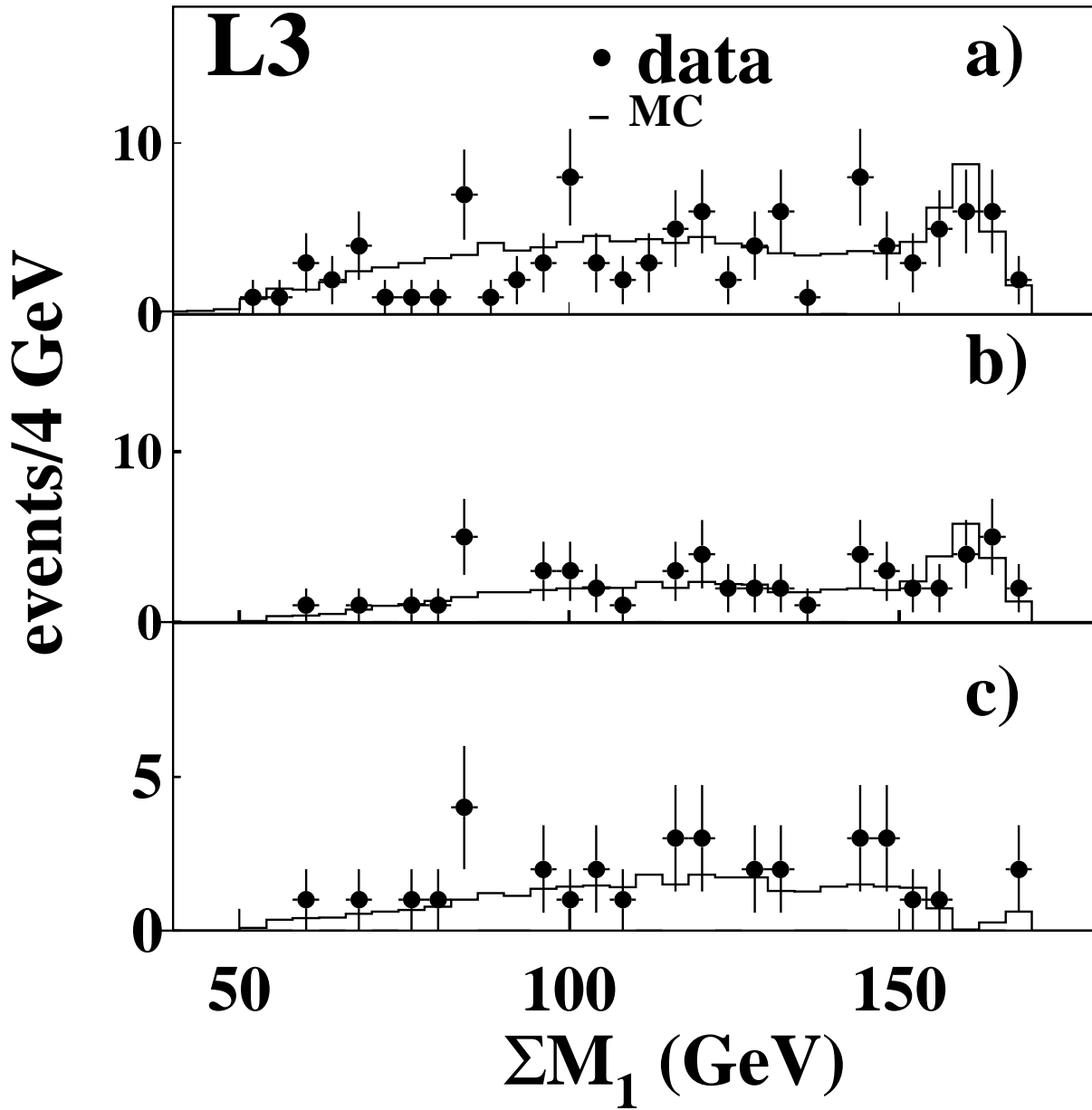


Figure 1: Distribution of the sum of the masses for the smallest difference (ΣM_1) at different stages of the analysis: (a) after the requirement of four jets, (b) after the requirements on kinematics and (c) after all cuts. Histograms are the expectations from the Standard Model while the dots are the data collected at $\sqrt{s} = 130 - 172$ GeV.

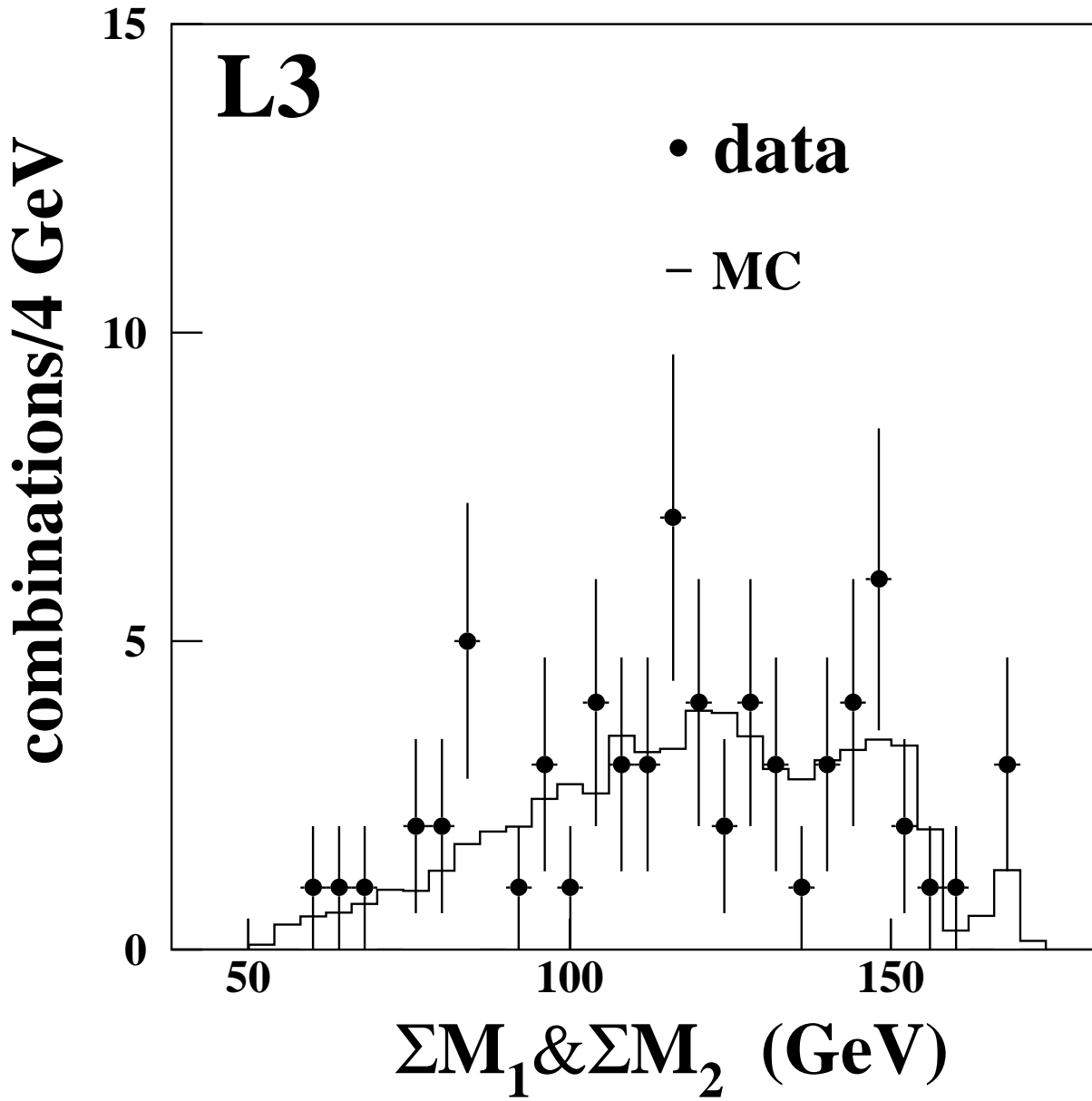


Figure 2: Distribution of the sum of the masses for the two smallest combinations (ΣM_1 and ΣM_2) together (two entries per event) after the selection. The whole data set collected at $\sqrt{s} = 130 - 172$ GeV is used.

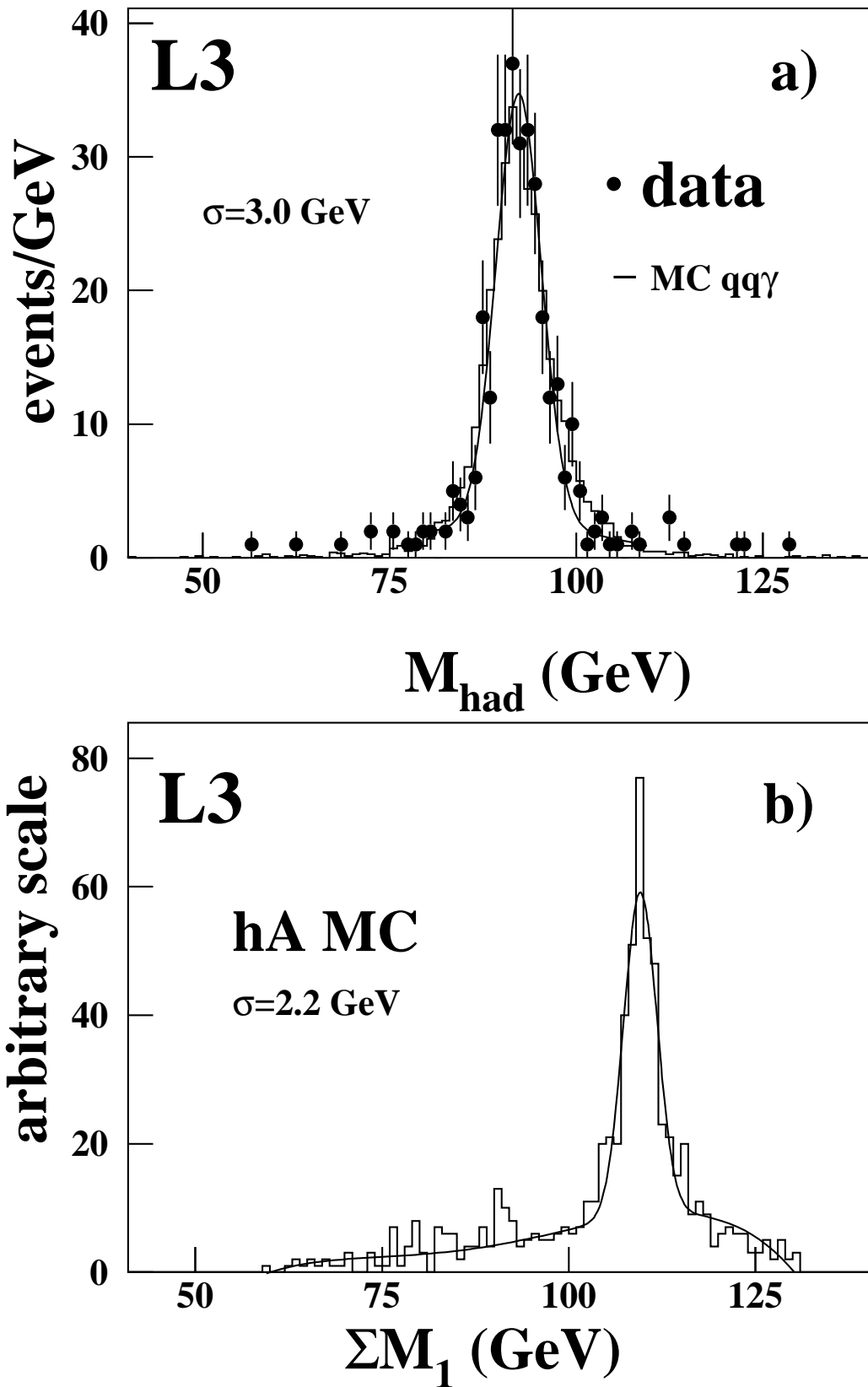


Figure 3: (a) Distribution of the reconstructed Z mass in $q\bar{q}\gamma$ events for data and MC at $130 < \sqrt{s} < 172$ GeV. (b) Spectrum of ΣM_1 for an $e^+e^- \rightarrow hA$ MC sample with $M_A = M_h = 55$ GeV at $\sqrt{s} = 133$ GeV.

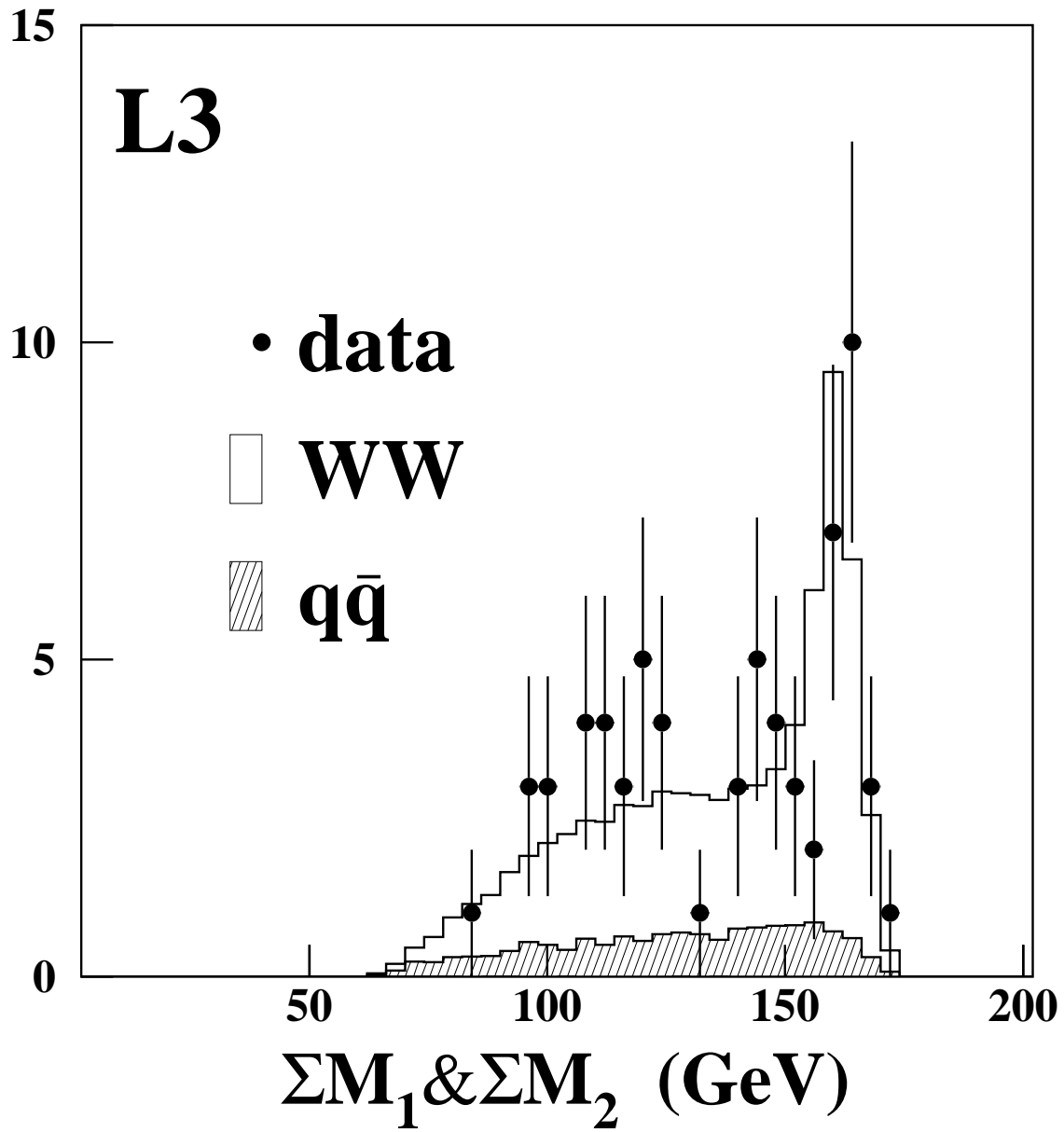


Figure 4: Distribution of ΣM_1 and ΣM_2 at $\sqrt{s} = 172$ GeV before the WW rejection is applied.

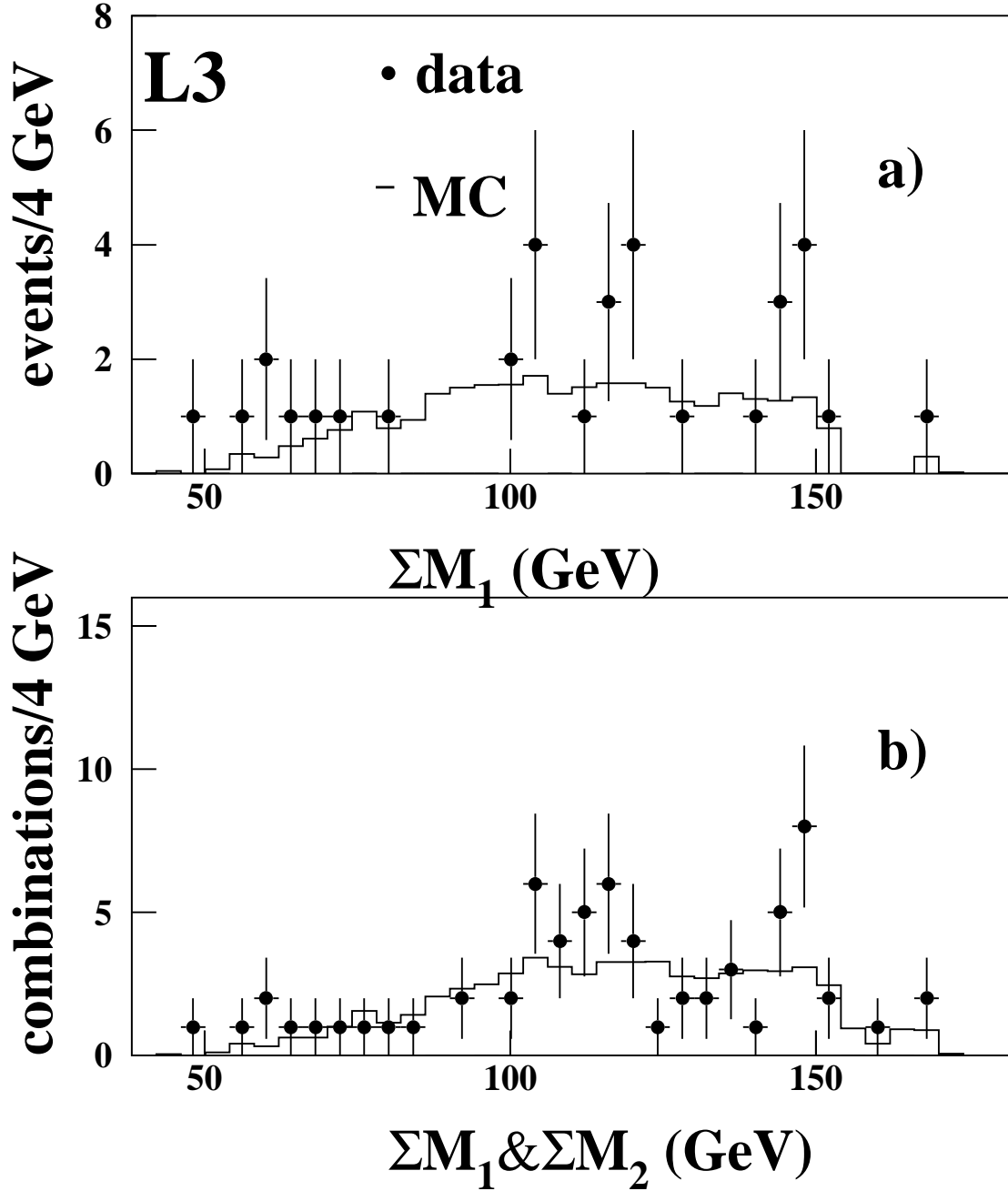


Figure 5: (a) Distribution of ΣM_1 and (b) of ΣM_1 and ΣM_2 with two entries per event obtained in the complementary analysis described in section 3.2. The data from $\sqrt{s} = 130$ to 172 GeV are combined.

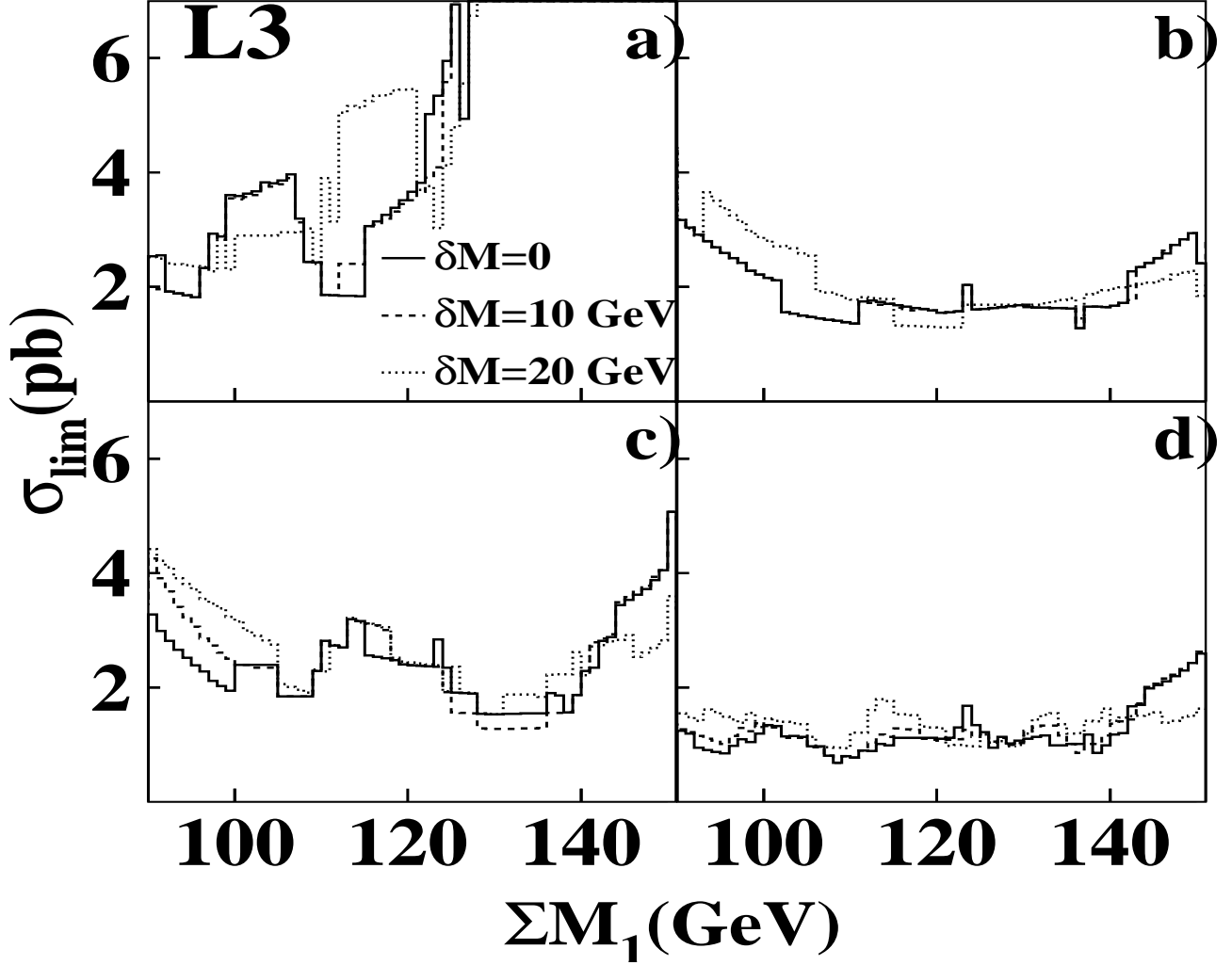


Figure 6: Maximum cross section (σ_{lim}) of a possible signal compatible with observations at 95% C.L. as a function of the sum of the masses ΣM_1 : a) $\sqrt{s} = 133$ GeV, b) $\sqrt{s} = 161$ GeV, c) $\sqrt{s} = 172$ GeV and d) combination of the three center-of-mass energies assuming a cross section constant with energy. Three different hypothesis are considered: the difference between the masses of the two bosons produced being 0, 10 or 20 GeV.